Research Article | Vol. 25, No. 20 | 2 Oct 2017 | OPTICS EXPRESS 24157
Optics EXPRESS

Tapered silicon core fibers with nano-spikes for optical coupling via spliced silica fibers

HAONAN REN,[1] OZAN AKTAS,[1,*] YOHANN FRANZ,[1] ANTOINE F. J. RUNGE,[1] THOMAS HAWKINS,[2] JOHN BALLATO,[2] URSULA J. GIBSON,[3,4] AND ANNA C. PEACOCK[1]

[1]*Optoelectronics Research Centre, University of Southampton, Southampton, SO17 1BJ, UK*
[2]*Center for Optical Materials Science and Engineering Technologies (COMSET) and Department of Materials Science and Engineering, Clemson University, Clemson, SC 29634, USA*
[3]*Department of Physics, Norwegian University of Science and Technology, 7491 Trondheim, Norway*
[4]*Applied Physics Department, KTH Royal Institute of Technology, SE-10691 Stockholm, Sweden*
**O.Aktas@soton.ac.uk*

Abstract: Reported here is the fabrication of tapered silicon core fibers possessing a nano-spike input that facilitates their seamless splicing to conventional single mode fibers. A proof-of-concept 30 µm cladding diameter fiber-based device is demonstrated with nano-spike coupling and propagation losses below 4 dB and 2 dB/cm, respectively. Finite-element-method-based simulations show that the nano-spike coupling losses could be reduced to below 1 dB by decreasing the cladding diameters down to 10 µm. Such efficient and robust integration of the silicon core fibers with standard fiber devices will help to overcome significant barriers for all-fiber nonlinear photonics and optoelectronics.

OCIS codes: (060.1810) Buffers, couplers, routers, switches, and multiplexers; (060.2280) Fiber design and fabrication; (060.2310) Fiber optics; (060.2290) Fiber materials; (160.6000) Semiconductor materials.

References and links

1. A. C. Peacock, U. J. Gibson, and J. Ballato, "Silicon optical fibres – past, present, and future," Adv. Phys.: X **1**, 114–127 (2016).
2. J. Ballato, T. Hawkins, P. Foy, R. Stolen, B. Kokuoz, M. Ellison, C. McMillen, J. Reppert, A. M. Rao, M. Daw, S. R. Sharma, R. Shori, O. Stafsudd, R. R. Rice, and D. R. Powers, "Silicon optical fiber," Opt. Express **16**(23), 18675–18683 (2008).
3. P. J. A. Sazio, A. Amezcua-Correa, C. E. Finlayson, J. R. Hayes, T. J. Scheidemantel, N. F. Baril, B. R. Jackson, D.-J. Won, F. Zhang, E. R. Margine, V. Gopalan, V. H. Crespi, and J. V. Badding, "Microstructured optical fibers as high-pressure microfluidic reactors," Science **311**(5767), 1583–1586 (2006).
4. B. L. Scott, K. Wang, and G. Pickrell, "Fabrication of n-type silicon optical fibers," IEEE Photonics Technol. Lett. **21**(24), 1798–1800 (2009).
5. C. Hou, X. Jia, L. Wei, S.-C. Tan, X. Zhao, J. D. Joannopoulos, and Y. Fink, "Crystalline silicon core fibres from aluminium core preforms," Nat. Commun. **6**, 6248 (2015).
6. H. El Hamzaoui, G. Bouwmans, B. Capoen, N. Chen, M. Douay, and M. Bouazaoui, "Sol–gel silica glass cladding semiconductor-core optical fiber," Mater. Today Commun. **11**, 179–183 (2017).
7. P. Mehta, N. Healy, T. D. Day, J. R. Sparks, P. J. A. Sazio, J. V. Badding, and A. C. Peacock, "All-optical modulation using two-photon absorption in silicon core optical fibers," Opt. Express **19**(20), 19078–19083 (2011).
8. R. He, P. J. A. Sazio, A. C. Peacock, N. Healy, J. R. Sparks, M. Krishnamurthi, V. Gopalan, and J. V. Badding, "Integration of gigahertz-bandwidth semiconductor devices inside microstructured optical fibres," Nat. Photonics **6**(3), 174–179 (2012).
9. Y. P. Huang and L. A. Wang, "In-line silicon Schottky photodetectors on silicon cored fibers working in 1550 nm wavelength regimes," Appl. Phys. Lett. **106**(19), 191106 (2015).
10. F. A. Martinsen, B. K. Smeltzer, M. Nord, T. Hawkins, J. Ballato, and U. J. Gibson, "Silicon-core glass fibres as microwire radial-junction solar cells," Sci. Rep. **4**(1), 6283 (2014).
11. S. Morris, T. Hawkins, P. Foy, J. Hudson, L. Zhu, R. Stolen, R. Rice, and J. Ballato, "On loss in silicon core optical fibers," Opt. Mater. Express **2**(11), 174510 (2012).
12. N. Gupta, C. McMillen, R. Singh, R. Podila, A. M. Rao, T. Hawkins, P. Foy, S. Morris, R. Rice, K. F. Poole, L. Zhu, and J. Ballato, "Annealing of silicon fibers," J. Appl. Phys. **110**(9), 093107 (2011).

#302001 https://doi.org/10.1364/OE.25.024157
Journal © 2017 Received 10 Jul 2017; revised 29 Aug 2017; accepted 2 Sep 2017; published 22 Sep 2017

Optics EXPRESS

13. S. Chaudhuri, J. R. Sparks, X. Ji, M. Krishnamurthi, L. Shen, N. Healy, A. C. Peacock, V. Gopalan, and J. V. Badding, "Crystalline silicon optical fibers with low optical loss," ACS Photonics **3**(3), 378–384 (2016).
14. N. Healy, M. Fokine, Y. Franz, T. Hawkins, M. Jones, J. Ballato, A. C. Peacock, and U. J. Gibson, "CO_2 laser-induced directional recrystallization to produce single crystal silicon-core optical fibers with low loss," Adv. Opt. Mater. **4**(7), 1004–1008 (2016).
15. Y. Franz, A. F. J. Runge, H. Ren, N. Healy, K. Ignatyev, M. Jones, T. Hawkins, J. Ballato, U. J. Gibson, and A. C. Peacock, "Material properties of tapered crystalline silicon core fibers," Opt. Mater. Express **7**(6), 2055–2061 (2017).
16. C. McMillen, G. Brambilla, S. Morris, T. Hawkins, P. Foy, N. Broderick, E. Koukharenko, R. Rice, and J. Ballato, "On crystallographic orientation in crystal core optical fibers II: Effects of tapering," Opt. Mater. **35**(2), 93–96 (2012).
17. F. H. Suhailin, L. Shen, N. Healy, L. Xiao, M. Jones, T. Hawkins, J. Ballato, U. J. Gibson, and A. C. Peacock, "Tapered polysilicon core fibers for nonlinear photonics," Opt. Lett. **41**(7), 1360–1363 (2016).
18. M. Wood, P. Sun, and R. M. Reano, "Compact cantilever couplers for low-loss fiber coupling to silicon photonic integrated circuits," Opt. Express **20**(1), 164–172 (2012).
19. S. McNab, N. Moll, and Y. Vlasov, "Ultra-low loss photonic integrated circuit with membrane-type photonic crystal waveguides," Opt. Express **11**(22), 2927–2939 (2003).
20. S. Xie, F. Tani, J. C. Travers, P. Uebel, C. Caillaud, J. Troles, M. A. Schmidt, and P. St. J. Russell, "As_2S_3-silica double-nanospike waveguide for mid-infrared supercontinuum generation," Opt. Lett. **39**(17), 5216–5219 (2014).
21. N. Granzow, M. A. Schmidt, W. Chang, L. Wang, Q. Coulombier, J. Troles, P. Toupin, I. Hartl, K. F. Lee, M. E. Fermann, L. Wondraczek, and P. S. Russell, "Mid-infrared supercontinuum generation in As_2S_3-silica "nano-spike" step-index waveguide," Opt. Express **21**(9), 10969–10977 (2013).
22. J.-H. Chen, Y.-T. Sun, and L. A. Wang, "Reducing splicing loss between a silicon-cored optical fiber and a silica optical fiber," IEEE Photonics Technol. Lett. **28**(16), 1774–1777 (2016).
23. E. F. Nordstrand, A. N. Dibbs, A. J. Eraker, and U. J. Gibson, "Alkaline oxide interface modifiers for silicon fiber production," Opt. Mater. Express **3**(5), 651–657 (2013).
24. J. Ballato, T. Hawkins, P. Foy, S. Morris, N. K. Hon, B. Jalali, and R. Rice, "Silica-clad crystalline germanium core optical fibers," Opt. Lett. **36**(5), 687–688 (2011).

1. Introduction

Over the past decade, the field of silicon photonics has benefitted from significant progress in the development of a wide range of novel waveguide devices, in both planar and fiber form [1]. As a material of choice for the fiber core, leveraging its both electronic and optical properties, silicon is predicted to establish the basis of various nonlinear photonic and optoelectronic devices. To date, two fabrication methods for silicon core optical fibers (SCF) have been developed: (i) molten core fiber drawing [2] and (ii) high pressure assisted microfluidic chemical deposition inside silica capillaries [3]. Of these, the former is the more globally practiced, which now includes several variations on this theme, such as drawing of powder-in-tube-type preforms [4], reactive aluminum core inside a silica cladding [5], and glass preforms prepared by sol-gel methods [6]. Several SCF-based devices also have been demonstrated for nonlinear optical and optoelectronics applications such as all-optical modulation [7], photodetection [8,9], and solar cells [10].

However, before the full potential of SCFs can be realized, there are two key hurdles that must be overcome: (i) reducing their optical transmission losses and (ii) establishing a method for robust integration with standard fiber infrastructure. Investigations of the sources of optical losses in as-drawn SCFs have revealed that material absorption due to impurities, scattering from grain boundaries and density fluctuations in the core make major contributions [11]. Several approaches have been employed to improve the material quality of the as-drawn fibers, such as photo-thermal processing [12], thermal annealing [13], and laser recrystallization [14]. Linear losses as low as 1 dB/cm have since been reported and are rapidly improving. Comprehensive material and structural characterization of the tapered SCFs has shown that the tapering process can also act to enhance the crystalline quality of the core through increasing the grain sizes [15] and aligning the crystallographic orientation with the fiber axis [16]. In addition, tapering has been utilized to decrease core diameters of as-produced SCFs down to sub-micron scales for dispersion engineering and mode field area reduction in nonlinear optical applications [17].

Optics EXPRESS

Today, a challenging problem hindering the technological exploitation of SCFs is the absence of a robust method for efficient optical coupling into micrometer-sized silicon cores. Free space coupling even with the highest numerical aperture objective lens is not efficient enough to couple light into subwavelength-sized silicon cores due to diffraction limited focusing and high Fresnel reflection at the silicon/air interface. Similar to the nano-tapers commonly used in planar silicon waveguides [18] and photonic crystal waveguides [19], inverse tapering of an As_2S_3 (n = 2.4) core inside a silica clad fiber has been utilized to achieve free space optical coupling with a loss of 2 dB [20] and supercontinuum generation [21]. Direct splicing of silica-clad SCFs to conventional single mode fibers (SMFs) has also been demonstrated [9], and micro-structuring of the silicon core surface via chemical etching before splicing has been proposed to reduce Fresnel reflection [22]. However, these methods still suffer from high losses due to mode field area mismatch, misalignment of the cores, and fragility of the splice joint due to the different thermal properties of the materials.

This paper reports the fabrication of tapered SCFs with nano-spikes that enable efficient optical coupling into the silicon core, as well as their robust integration to SMFs by splicing. A proof-of-concept 30 µm cladding diameter SMF-SCF device is demonstrated. Optical characterization is performed using the cut-back method to measure propagation and spike coupling losses, which are below 2 dB/cm and 4 dB, respectively. Moreover, we investigate the potential of coupling via nano-spikes into micron-sized silicon cores by finite-element-method-based simulations, which show that the coupling losses could be reduced to below 1 dB if the cladding diameters are decreased to 10 µm. The nano-spikes are convenient in terms of damage threshold, because high optical power couples into the core gradually over the large-area nano-spike surface rather than abruptly at the flat surface of an interface.

2. Fabrication and integration

The SCFs used in this work were fabricated using the molten core fiber drawing technique. Fabrication of the preform is detailed in [10]. A thin layer of calcium oxide (CaO) was first coated inside the silica capillary tube to prevent oxygen in-diffusing during the process. This coating, which is a mixture of CaO and SiO_2 [23], also serves as an intermediate index cladding (IIC) and stress-reducing layer. A phosphorus doped silicon rod (0.13-0.145 ohm-cm) was then sleeved into the silica tube and was drawn into a fiber using standard fiber drawing process at a temperature of 1950°C, which produced many meters of SCFs with continuous silicon cores as small as 5 µm in diameter. As-drawn SCFs are poly-crystalline, and have high tensile stress due to the large difference in the thermal expansion coefficients of silica and silicon. This tensile stress can be used to create a void gap by melting the core locally with a heat-polishing method based on unidirectional movement of the as-drawn fiber in a hot zone, as shown schematically in Fig. 1(a). Tapering of the fiber with the void gap is performed by slowly feeding the fiber into the hot zone and pulling it from the other end with a higher pulling speed (see Fig. 1(b)). Collapsing of the void gap results in a silicon-free region with a CaO/SiO_2 core, and a silicon nano-spike at the right end. After cleaving the tapered SCF at the silicon-free region, a tapered SMF can be spliced to this facet, as shown in Figs. 1(c) and 1(d). An integrated fiber device (see Fig. 1(e)) is finally obtained releasing the tapered SCF after cleaving.

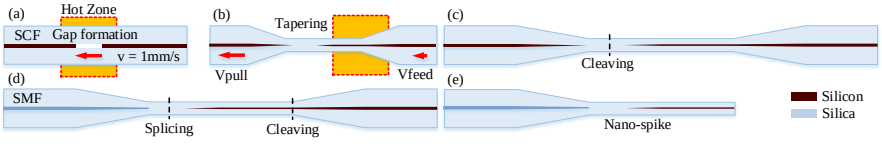

Fig. 1. Steps of fabrication. (a) Void gap formation in the core of an as-drawn SCF after heat-polishing process. (b) Tapering of the void gap in the core results in a silicon-free region with a CaO/SiO_2 core, and a nano-spike. (c) Cleaving of the tapered SCF. (d) Splicing the SCF with a tapered SMF and final cleaving at the other end. (e) An SMF-SCF device with a nano-spike.

Optics EXPRESS

In order to fabricate a SMF-SCF device, a glass processing system (Vytran GPX-3400-V4) conventionally employed for SMFs was used for heat-polishing, tapering, and splicing. An as-drawn SCF with clad/core diameter of 144/5.5 μm was first loaded under 30 g tension on two motorized stages and heat-polished by moving the fiber over a 3 mm range at a rate of 1 mm/s, inside a 2 mm wide electrically heated (55 W) graphite filament (V4) at a temperature slightly above the melting point of silicon (T_m = 1414°C). A ~150 μm long void gap was created in the silicon core, as shown in Fig. 2(a), due to release of the built-in tensile stress. An IIC layer can be seen as a darker annular region around the void core for a SCF cleaved at the gap, as shown in Fig. 2(b). The IIC layer is assumed to have a refractive index of 1.6, i.e., average of CaO and SiO_2. The thickness of the IIC layer is around 1.25 μm.

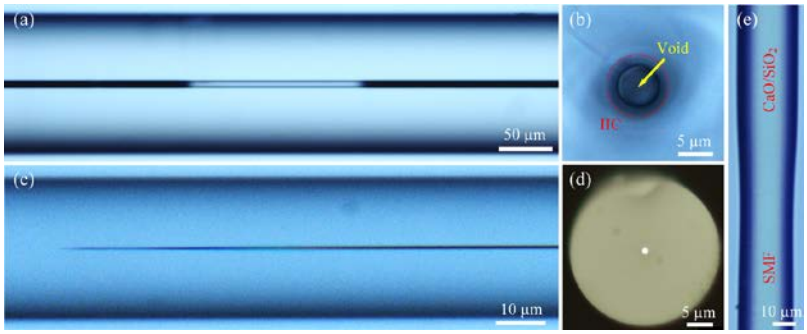

Fig. 2. Optical microscopy images show (a) an as-drawn SCF with a void gap in the silicon core created by heat-polishing, (b) an intermediate index cladding (IIC) layer of CaO/Silica (inside the red circle) around the void core, (c) a nano-spike produced after SCF tapering, (d) the cleaved end facet of the tapered SCF for output coupling, and (e) the splice joint.

After the formation of a void gap in the core, the SCF was directly tapered with a ratio of 144:30 to form a 15 mm long waist region between two 10 mm long transition regions. The power (68 W) applied to the heating element in the glass processing system was adjusted such that the resultant temperature exceeded the softening point of the silica. In this case, tapering of the SCF collapsed the IIC layer surrounding the void gap forming a CaO/SiO_2 core in the center of the 30 μm waist and creating a sharp silicon nano-spike, as shown in Fig. 2(c). The nano-spike was encapsulated by the IIC layer, which is estimated to be around 260 nm in thickness given the tapering ratios. The tapered SCF was then cleaved to obtain a facet that was clean and flat, as shown in Fig. 2(d), at a point 2 mm away from the nano-spike to protect it from high temperatures during the subsequent splicing of the tapered SCF with an adiabatically tapered SMF. The SMF was tapered so that the core guided mode transitioned into the cladding guided mode propagating within the waist region, which had almost the same diameter as the tapered SCF. Splicing of the tapered SCF to the tapered SMF (see Fig. 2(e)) was achieved by applying a heating power of 63 W over 7 seconds. Finally, the tapered SCF was cleaved again on the other end, releasing a device with a 1.1/30 μm core/cladding diameter SCF of 12 mm length and a 200 μm long nano-spike, as measured via optical microscopy and scanning electron microscopy (SEM) following HF etching of the silica cladding. A larger cladding diameter SCF can be fabricated with a nano-spike by using the same method, however, careful consideration must be applied to avoid compromising the coupling efficiency.

3. Simulations

FEM-based simulations were used to calculate optical coupling losses of the nano-spike for different cladding diameters (D = 10-30 μm) and IIC layer thicknesses (h = 0-400 nm) at λ = 1550 nm, using COMSOL software. The nano-spike starts from 5 nm in diameter and widens to a core diameter of 1 μm at the end of the transition length of 200 μm. A section of fiber with a CaO/SiO_2 core was placed before the nano-spike and a silicon core was placed after,

Optics EXPRESS

both of which had a constant diameter and a length of 50 µm. Material absorption was assumed to be zero to investigate only the effects of dimension change on coupling losses.

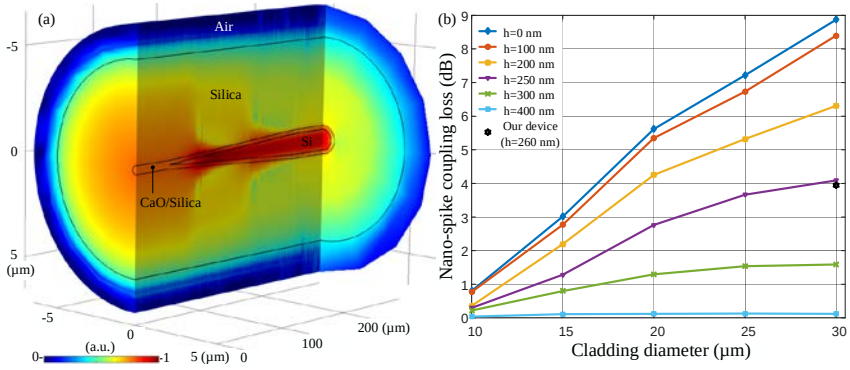

Fig. 3. (a) Simulation of light coupling into a silicon core via the nano-spike encapsulated with an intermediate index (n = 1.6) cladding layer of thickness h = 200 nm and a cladding diameter of 10 µm. Spike coupling loss is 0.35 dB for this geometry. Electric field strength is shown in normalized logarithmic scale (a.u.). (b) Spike coupling loss versus cladding diameter for various IIC layer thicknesses h, and our device which is designated with a star.

For the initial case where the IIC layer thickness was taken as h = 0 nm, optical coupling from the cladding guided fundamental mode of a tapered SMF to the fundamental mode of a SCF via the silicon nano-spike was simulated to estimate spike coupling losses for different silica cladding diameters D. For IIC layer thicknesses h > 0 nm, a spike encapsulating layer with a refractive index of 1.6 was used to calculate coupling losses from the fundamental mode of a CaO/SiO_2 core (n = 1.6, r = h) to the fundamental mode of a SCF. The spike coupling loss was calculated to be 0.35 dB for a SCF with a cladding diameter of 10 µm and a core diameter of 1 µm. The profile of the electric field strength through the fiber is shown in Fig. 3(a) for these parameters. Presence of the IIC layer improves optical coupling to the high index (n = 3.48) silicon nano-taper, as shown in Fig. 3(b). However, in addition to the nano-spike coupling losses, mode conversion losses between the tapered SMF and the CaO/SiO_2 core fiber at the splicing point can also increase up to 3 dB for thicker IIC layers (h ≥ 300 nm). Nevertheless, both of the coupling and mode conversion losses can be reduced to below 1 dB by decreasing the silica cladding diameter D below10 µm and the IIC layer thickness h below 100 nm. With the numerical parameters set to those of our experimental SMF-SCF device, the nano-spike coupling loss and the mode conversion loss at the splice point are calculated to be 3.9 dB and 1.25 dB, respectively. For the mode conversion loss calculation, all parts of the device, i.e., SMF, CaO/SiO_2 section and Si nano-spike, were taken into account. Previously, coupling of a tapered SMF to a planar Si waveguide with an inverse nano-taper was demonstrated with coupling losses below 1 dB for both TM- and TE-like modes at λ = 1550 nm [18], using a silica cladding width of 2 µm. SCFs can potentially achieve similar low coupling losses with less fabrication complexity, but higher robustness.

4. Optical characterizations

Optical characterization of the SMF-SCF device is schematically shown in Fig. 4(a). The SMF-SCF device under test was connected to an infrared continuous-wave (CW) laser (Tunics T100S-HP) with a fiber coupled output of 1mW at λ = 1550 nm and a 63x objective lens with a NA of 0.85 to collect the output power from the cleaved facet. The output mode is a superposition of cladding guided and core guided modes as can be seen from the image in Fig. 4(b), taken by an IR camera (Micronviewer 7290a). The simulated power profile of the output mode for the device is also shown in Fig. 4(c). A pinhole was used to filter the cladding mode so that only the core mode remained for the power measurement. The output mode profiles measured by a beam profiler (Spiricon) before and after spatial filtering are

Optics EXPRESS

shown in Figs. 4(d) and 4(e), respectively. The power was measured at 5 different cut-back positions along the device as shown in the inset of Fig. 4(f).

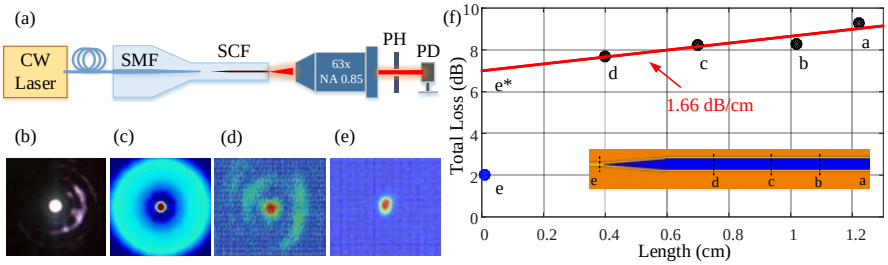

Fig. 4. (a) Optical characterization setup. (b) IR camera image of the output mode. (c) Simulated power profile of the output mode. (d) Experimental output mode profile image taken by a beam profiler. (e) Output mode profile after spatial filtering. (f) Loss measurements with a linear fit to the data. Inset shows the cut-back positions. PH = Pinhole, PD = Photodetector.

Initially, the total transmitted power was 330 µW. After spatial filtering, the power of the core guided mode was measured to be 118 µW at position *a*, which corresponds to a total loss of 9.2 dB. A linear fit to the cut-back data was used to calculate a propagation loss of 1.66 ± 0.54 dB/cm, which is slightly lower than our previously reported loss of 2 dB/cm for SCFs [15]. The uncertainty in the measurements occurs due to the slight changes in the angle of cleaving, the surface quality, and the output coupling condition. At each cut-back position, we have also observed a ~5% variation in the core diameter (1.1 µm), which is in the resolution limit of the optical microscopy. The losses due to these variations are included in the total loss. After the nano-spike was removed at position *e*, a loss of 2 dB was measured, which includes fiber connector loss, SMF tapering loss, and the mode conversion loss at the splicing point (estimated to be 1.25 dB from the simulations). The estimated loss of the device (7 dB) at the nano-spike input was determined from the y-intercept of the linear fit. The difference between this estimated loss at position *e** and the measured loss at position *e* gives a total coupling loss of ~5 dB at the nano-spike, which includes the nano-spike coupling loss as well as an extra loss due to the change of interface from Si-air (~1.5 dB) to CaO/SiO_2-air (~0.2 dB) at the position *e*. Accounting for this extra loss, the nano-spike coupling loss was estimated to be ~3.7 dB, which is in accordance with the simulated value of 3.9 dB. Both of the nano-spike coupling and mode conversion losses could be reduced to below 1 dB by decreasing the silica cladding diameters ($D \leq 10$ µm) and the thickness of the IIC layer ($h \leq$ 100 nm), respectively. Further improvement in material quality of the tapered SCFs similar to the results [12–14], can mitigate propagation losses below 1 dB/cm. Formation of the nano-spikes in the core of silica fibers can also be achieved with other semiconductors such as germanium [24] or glasses with melting temperatures lower than the softening point of silica.

5. Conclusion

Reported here was the fabrication of tapered SCFs with nano-spikes and their robust integration with SMFs by splicing. Loss measurements have revealed the propagation and nano-spike coupling losses for our 30 µm cladding diameter device to be below 2 dB/cm and 4 dB, respectively. Theoretical nano-spike coupling losses are below 1 dB for cladding diameters $D \leq 10$ µm. Seamless integration of SMFs and SCFs can pave the way for photonic and optoelectronic devices such as SCF Raman amplifiers and fiber photodetectors.

Funding

The Engineering and Physical Sciences Research Council (EPSRC) (EP/P000940/1).

Optics EXPRESS

Acknowledgments

The authors wish to acknowledge financial support from the Norwegian Discovery Fund, NORFAB and the J.E. Sirrine Foundation. All data supporting this study are openly available from the University of Southampton repository at http://doi.org/10.5258/SOTON/D0211